PHASE RELATIONSHIPS AND FRACTIONATION IN MULTICOMPONENT POLYMER SOLUTIONS*

R. KONINGSVELD

Centraal Laboratorium, DSM, Geleen, The Netherlands

1. INTRODUCTION

Phase separation of polymer solutions has long been used as a tool in fractionating polymers according to molecular weight. In a two-phase system the distribution of the macromolecules between the phases is governed to a large extent by their chain length. This is apparent when such systems, whether or not in equilibrium, are subjected to a liquid–liquid or a liquid–polymer crystal separation. In the present paper we shall deal only with liquid–liquid separations, carried out in two-phase systems which are in equilibrium. The polymers to be considered are homopolymers containing linear chains of different length.

The art of fractionation fundamentally amounts to finding the conditions under which the separation according to molecular weight will be as sharp as possible. The nature of the process is characterized by the tendency of all species in the polymer to distribute themselves between the two liquid phases. In an efficient fractionation the conditions must be so chosen that the amount of undesired components in one of the phases is minimised. However, no matter how carefully the fractionation is carried out, a separation into pure components is virtually impossible, and we must accept that even the purest fraction still contains many components.

This has consequences both in analytical and preparative fractionation work. The analytical aspect of fractionation, i.e. the determination of the molecular weight distribution curve from fractionation data, confronts us with a very old problem, which has been extensively studied[1–6]. We shall not go deeply into it here, but turn our attention primarily to the accuracy attainable. Of course, the analytical and preparative aspects have very much in common.

In preparative fractionation it is important not only to carry out the separation in such a way that a fraction with a narrow molecular weight distribution is obtained, but also to isolate a sufficient amount of this fraction to permit further investigation. With regard to the latter point we may say that a fraction size of about one hundred grammes would certainly not be too large. For preparing such an amount of well-fractionated material large quantities of initial polymer are needed; the order of magnitude can be estimated as follows.

Consider an exponential weight distribution:

$$w(M) = W\tau^{\lambda+2}[\Gamma(\lambda+2)]^{-1}M^{\lambda+1}\exp(-\tau M) \qquad (1)$$

* Plenary lecture presented at the 3rd Microsymposium 'Distribution Analysis and Fractionation of Polymers', held in Prague, Czechoslovakia, during 23–26 September 1968.

where $w(M)$ = the mass of molecules with molecular weight M,
W = the total mass of polymer,
Γ = the gamma function,
λ = $(2-b)/(b-1)$,
τ = $(\lambda+1)/M_n$,
b = M_w/M_n,
M_w = $\int_0^\infty Mw(M)\mathrm{d}M/W$ = the weight-average molecular weight,
M_n = $W/\int_0^\infty M^{-1}w(M)\mathrm{d}M$ = the number-average molecular weight.

The exponential function is a maximum at $M = M_n$.

Denoting the width of the distribution by b ($= M_w/M_n$), one might ask what will be the relation between the maximum possible yield of a fraction of a given M_n and its b-value. Obviously, one obtains the maximum fraction size at a given b-value if the number average molecular weight equals that of the original polymer (assuming an exponential fraction distribution). Then, we have the situation shown in *Figure 1*.

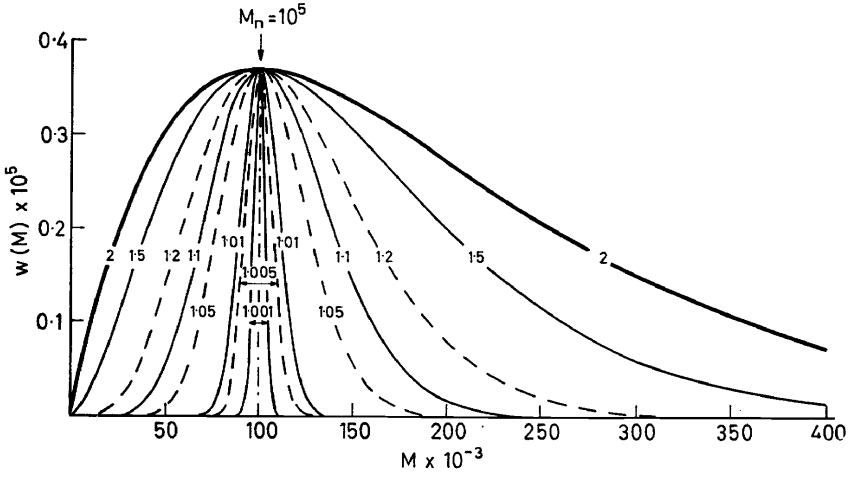

Figure 1. Exponential fraction distributions (b values indicated) allowing maximum yield from an exponential initial distribution ($b = M_w/M_n = 2$; $M_n = 10^5$).

Figures 2 and *3* show the dependence on the b-value of the fraction of the yield of fraction and the amount of initial polymer needed to obtain a 100 g fraction. As would be expected, the yield decreases considerably in the b-range of interest. The size of the polymer to be fractionated amounts to several kilogrammes.

In practical separation work, the maximum yield (coincident maxima of the distributions) is not readily obtained. On the other hand, as the initial M_n value decreases, the situation may become less unfavourable but, if we move away from the maximum or have a wider or different initial distribution or a higher M_n value, the yield may still be smaller than that in the present

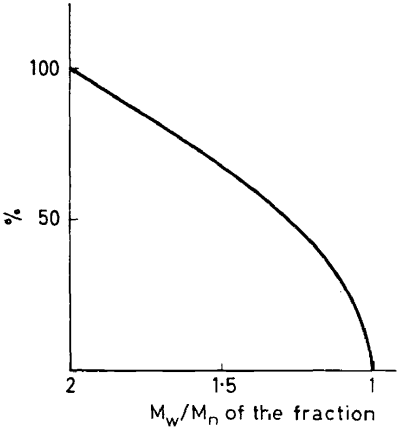

Figure 2. Maximum yield of fraction from an initial exponential distribution ($b = 2$; $M_n = 10^5$).

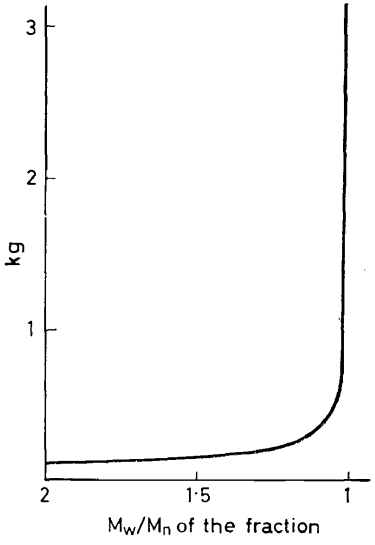

Figure 3. Amount of initial polymer (exponential distribution, $b = 2$, $M_n = 10^5$) needed for a 100 gram fraction at maximum yield.

example. Hence, the preparation of sufficient quantities of fractions with really narrow distributions will necessarily involve fractionation of several kilogrammes of polymer.

This requirement rules out all current fractionation methods except the classical precipitation and extraction techniques. Their principles are well-known[1–5]; in *fractional precipitation* one tries to increase the quantity of

the high-molecular-weight components in the concentrated phase, whilst decreasing the amount of low-molecular-weight constituents in this phase as much as possible. Conversely, with *extraction* one separates the low-molecular-weight components and tries to avoid high-molecular-weight contamination.

Before proceeding with a discussion of methods suited for practical large-scale separation work, it may be instructive to estimate whether the experimental efforts involved will bring us anywhere near the ultimate aim of fractionation: separation of pure components. Inspection of *Figure 1* reveals that, even at $b = 1{\cdot}001$, the half-width of the fraction distribution is still 7000, whereas the width at the base of the distribution is about 20000. With a monomer molecular weight equal to 100, this means that there are about 200 components, more than 70 of which are present in appreciable amounts. At $b = 1{\cdot}05$, which can be considered a very satisfactory fractionation result, these figures are about 1600 and 500, respectively.

2. LIQUID–LIQUID PHASE RELATIONSHIPS IN NON-BINARY MIXTURES

Graphical representation of two-liquid-phase relationships in binary systems does not present any problems. The number of degrees of freedom is two, and a planar diagram is adequate. The limit of visualizability is reached as soon as one more component is added, and multicomponent mixtures, like polymer solutions, compel us to turn to graphical representations, which may be ambiguous.

A consideration of ternary solutions containing a solvent and two macromolecular homologues brings out most of the deviations from truly binary phase diagrams, as are also to be expected with multicomponent systems. Very useful ternary diagrams have been calculated by Tompa[7], who used Flory[8,9] and Huggins[10,12] free enthalpy of mixing function (ΔG) for the purpose.

The free enthalpy (Gibbs free energy) governs the equilibrium behaviour of the system and it is therefore important to make an appropriate choice of the ΔG function. The expression derived by Flory and Huggins on the basis of the lattice theory might be considered too rough an approximation. More refined functions are indeed available[13–16]. However, the Flory–Huggins expression has been found suitable for describing phase relationships in a qualitative[7,9] and, occasionally, also in a quantitative way[17–22]. It offers a considerable advantage over the more refined functions in that it has a relatively simple form. For quantitative use, it may be necessary to assume the interaction parameter to be concentration-dependent.

Flory and Huggins' ΔG function reads:

$$\Delta G/RT = \phi_o \ln \phi_o + \Sigma \phi_i m_i^{-1} \ln \phi_i + g\phi_o\phi \qquad (2)$$

where ΔG = the free enthalpy of mixing per mole of lattice sites,
ϕ_o = the volume fraction of the solvent,
ϕ_i = the volume fraction of macromolecular species i,
$\phi = \Sigma\phi_i$ = the whole polymer volume fraction,

m_i = the chain length of species i, expressed as the number of lattice sites,

g = the interaction parameter[7,9,12]

The other symbols have the usual meaning.

Equilibrium conditions can be derived from Eq. (2) by equating the chemical potentials of the components in the two phases. This leads to a number of equations equal to the number of components. For the numerical solution of these equations the reader is referred to the relevant literature[17,18,23-25].

The miscibility gaps thus calculated by means of Eq. (2) have the asymmetric shape which, as found from experiment, is typical of polymer

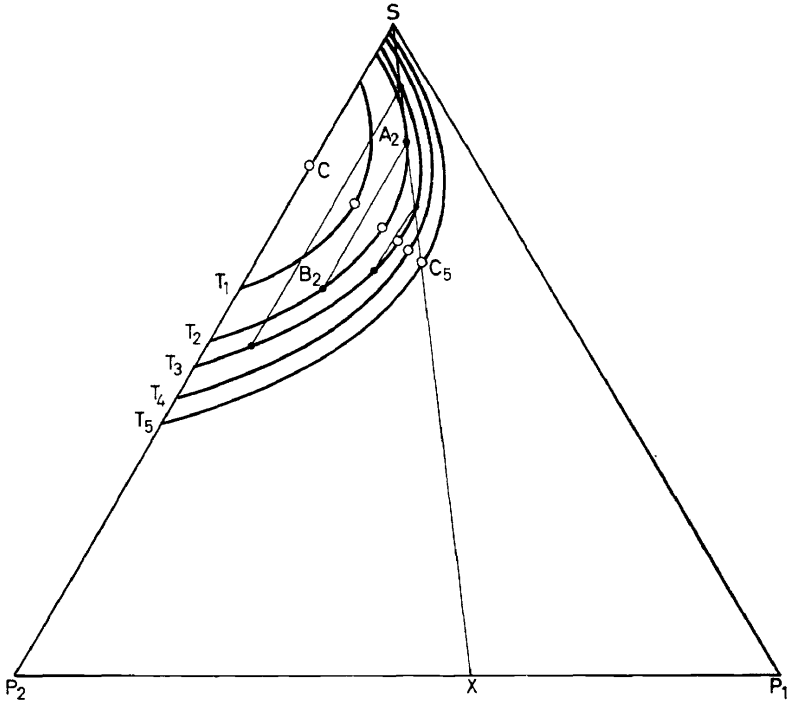

Figure 4. Ternary binodals for different temperatures. Critical points are denoted by circles. Tie lines are drawn in for T_2 and T_3. The chain length of P_2 is larger than that of its homologue P_1.

solutions[7-12]. A schematic illustration of Tompa's ternary examples is given in *Figure 4*, which shows the development of the immiscibility area upon a change in temperature. The two polymer homologues P_1 and P_2 differ in molecular weight ($M_2 > M_1$). Compositions of phases coexisting at a given temperature (e.g. A_2 and B_2 at T_2) are connected by tie lines. The latter

tend to shorten as the critical, or consolute point, where the two phases become identical, is approached.

All solutions of a mixture of P_1 and P_2, say X, in the single solvent S, are represented by points on SX. The extreme temperature at which a solution of X in S can show phase separation is T_2, and it should be noted that the system A_2 at this precipitation threshold—as it was called by Tompa[26]—is not in the consolute state, but on the contrary, coexists with B_2. This statement is valid irrespective of whether $T_1 > T_5$ or $T_5 > T_1$.

The isothermal locus of the coexisting or conjugate phases is called binodal. If the binodals for the various temperatures are put together in a three-dimensional diagram, we obtain *Figure 5*. This figure reveals the

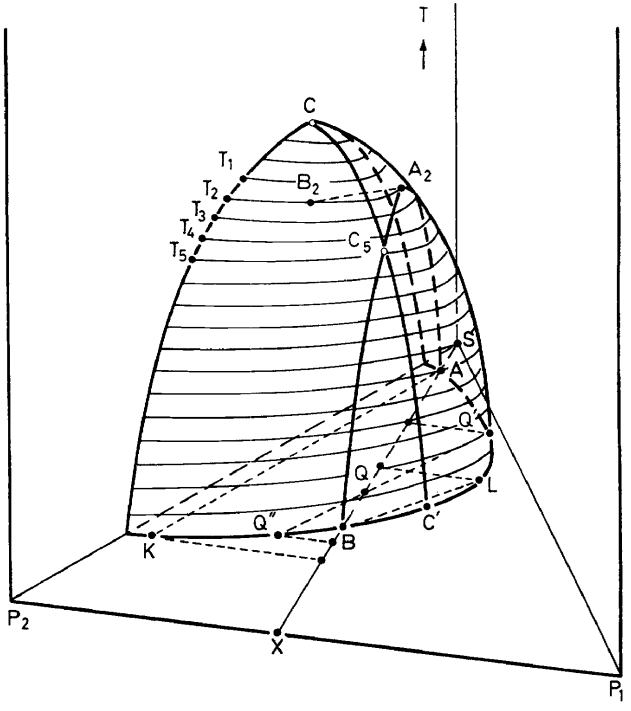

Figure 5. Miscibility gap in solutions of a binary polymer (components P_1 and P_2) in a single solvent S. AA_2C_5B: quasi-binary section (cloud-point curve); A_2: precipitation threshold; CC_5C': locus of critical points.

nature of the graph obtained by plotting the data of a series of cloud-point measurements on a planar diagram. Miscibility gaps in polymer solutions can often be measured conveniently by changing the temperature of homogeneous solutions of various concentrations, and noting the temperature at which demixing sets in (cloud-point). Plotting the observed cloud points against polymer concentration yields the cloud-point curve, which, in *Figure 5*, is identical to the quasi-binary section AA_2C_5B. In fact, if X represents the investigated polymer, the plane of our graph is TSX.

Unlike the behaviour observed in binary systems, such as SP_2, the cloud point curve AA_2C_5B does not represent coexisting phases, and its extreme (the precipitation threshold) is not a consolute point. The latter is indeed located on the curve, but must be sought at a higher polymer concentration. This can be conclusively proved[27,28].

Considering a system within the miscibility gap (Q), we find the two conjugate phases Q' and Q'' both outside the plane TSX. If we plot the overall polymer concentrations of the two phases, we actually project Q' and Q'' onto TSX. Doing so for different temperatures, we obtain a co-existence curve which comprises two branches, one referring to the dilute, the other to the polymer-rich phase. The two branches are not connected, unless the overall polymer concentration of system Q happens to equal the critical concentration corresponding to C_5[17,19,20].

The compositions of the phases coexisting with cloud-point systems (e.g. A, A_2, B and K, B_2, L, resp.) can also be projected onto TSX. The locus of the points thus obtained is the coexistence curve of the cloud-point curve. The former has been called the shadow curve, because it cannot be measured in a direct way[19]. As can be seen in *Figure 5* an increase of the overall concentration from A to B causes the two branches of the coexistence curve to move closer together. Instead of the single binodal in a truly binary system, we now have coexistence curves the location of which depends on the overall concentration. They are confined to the region between the cloud-point and the shadow curves[19].

All these different curves eventually coincide if we move X to P_2; this yields a binary mixture, in which, in conformity with the phase rule, the critical point is found at the extreme of the binodal. Upon shifting X, i.e. upon a change of the polymer composition, all phase relationships change, and the shape of the quasi-binary phase diagram must therefore be expected to vary with the polymer composition.

All the features referred to above are reflected in the phase behaviour of polymer solutions containing many more than three components. *Figure 6* shows some examples calculated on the basis of Eq. (2) with g independent of the polymer concentration ϕ. Because the $g(T)$ relation is left undefined, g instead of T appears on the ordinate.

For the purpose of calculation the molecular weight distribution of the polymer must be chosen. Distribution shapes differing from the exponential function (1) can be constructed either by suitable addition of two or more exponential functions[17,18], or by using, e.g. the logarithmic normal function:

$$w(M) = WbM_n^{-2}\beta^{-1}\pi^{-\frac{1}{2}}M \exp\left[-\beta^{-2} \ln^2 (M/M_o)\right] \qquad (3)$$

where $\beta^2 = 2 \ln b$,

$M_o = M_n b^{-1}$,[5]

The distribution functions used for *Figure 6*, and some others to be employed later, are shown in *Figure 7*. Their characteristics are listed in *Table 1*.

The most striking feature of *Figure 6* is the variation of the shape of the phase diagram with polymer composition. All three distributions are identical with respect to M_n and M_w, but M_z differs. The skewness of the distribution curve increases with M_z (*Figure 7b*) and so does the distortion of the phase diagram. All qualitative aspects observed in *Figures 4* and *5* are

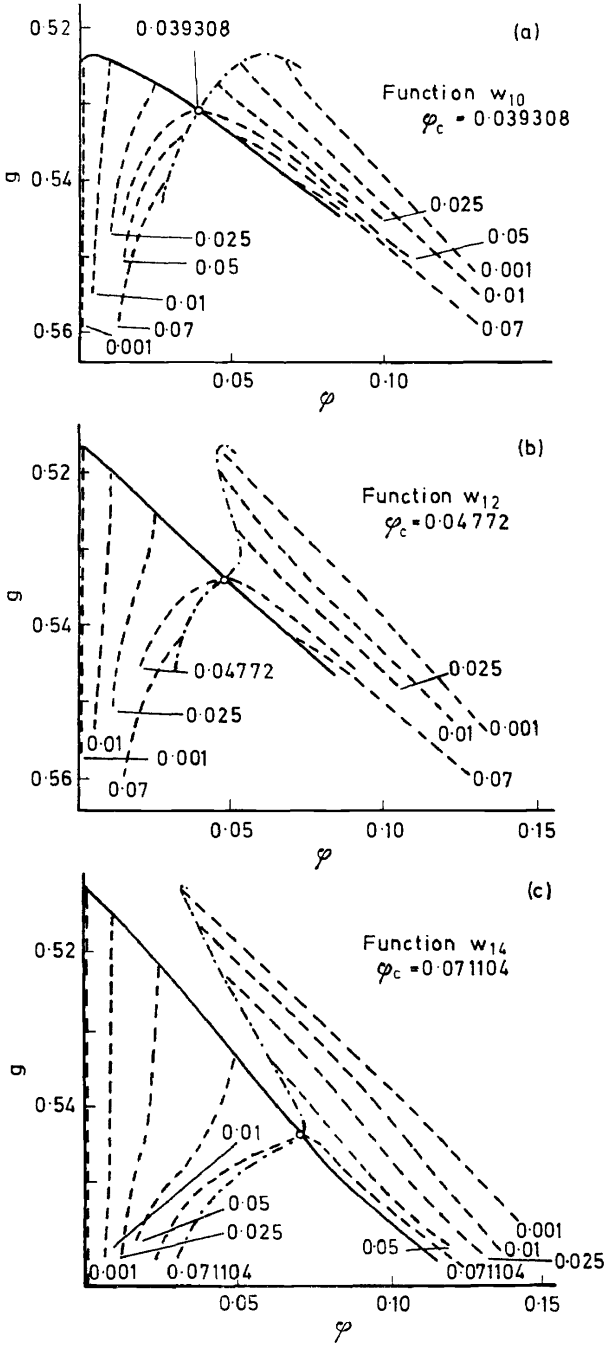

Figure 6. Planar phase diagrams for three molecular weight distributions. $M_w = 131{\cdot}7 \times 10^3$; $b = 5$. Cloud-point curve: ————; shadow curve: — · — · —. Coexistence curves for indicated values of overall polymer volume fraction ϕ: — — — —; critical point: 0.

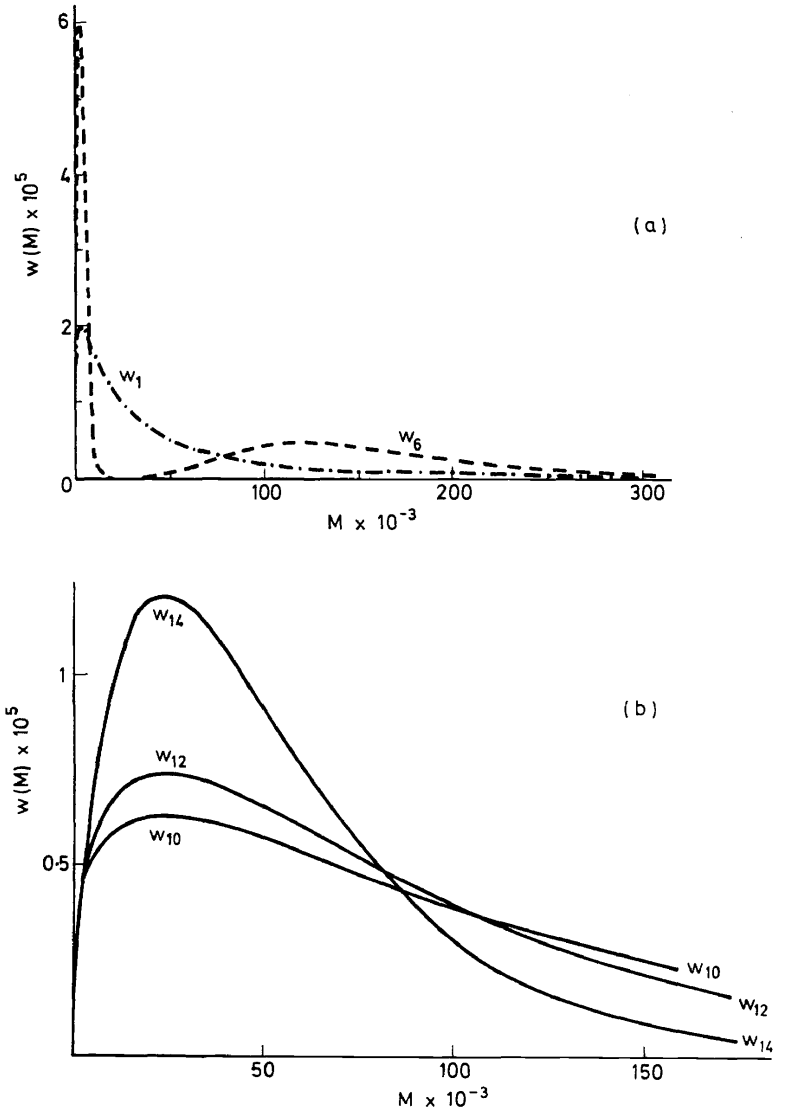

Figure 7. Some of the distribution functions used in the calculation of phase separations and fractionations.

also noted here. The change in M_z is one of the many multicomponent analogues of a shift of X on the P_1P_2 axis in *Figures 4* and *5*.

Experimental evidence demonstrates that the phenomena discussed here are real. Rehage *et al.*[29,30] measured phase relationships in solutions of a sample of polystyrene in cyclohexane. *Figure 8*, which is based on their results, brings out the qualitative confirmation. Further experimental data

Table 1. Characteristics of some of the model distribution functions

Function	*Type*	$M_w . 10^{-3}$	M_w/M_n	M_z/M_w
w_1	log normal function	131·7	10	10
w_2	log normal function	26·34	2	2
w_5	log normal function	131·7	2	2
w_6	sum of 2 log normal functions	131·7	10	1·64
w_7	exponential function	131·7	2	1·5
w_{10}	sum of 2 exponential functions	131·7	5	2
w_{12}	sum of 2 exponential functions	131·7	5	3
w_{14}	sum of 2 exponential functions	131·7	5	7
w_{15}	exponential function	125·6	1·13	1·115
w_{16}	sum of 2 exponential functions	125·0	1·25	1·12
w_{17}	sum of 2 exponential functions	12·5	1·25	1·12

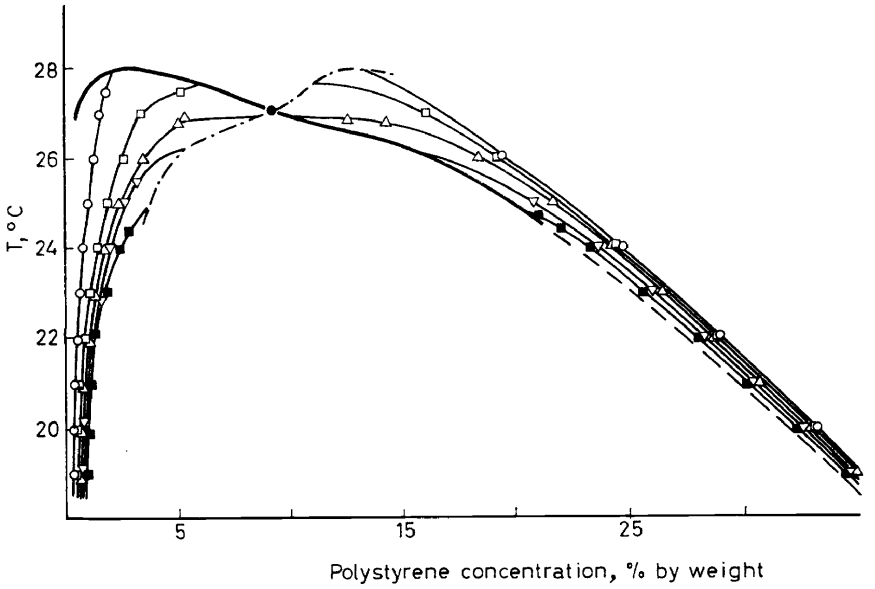

Figure 8. Quasi-binary phase diagram for solutions of a sample of polystyrene in cyclohexane. Data from Rehage *et al.*[29,30] Cloud-point curve: ———; coexistence curves at 2 (○), 6 (⊡), 10 (△), 15 (▽) and 20 (■) per cent overall concentration (per cent by weight): ———; shadow curve: — · — · —; critical point: ●.

have been collected on the system polyethylene–diphenylether[17,19]; *Figure 9* shows some results. In *Figure 10* it is seen that the actual phase behaviour may follow the calculated trends in detail. The calculated and measured dilute phase branches of the coexistence curves refer to quite comparable distributions and concentrations.

If the phase diagram and, hence, the compositions of the conjugate phases are so highly dependent on the polymer composition (molecular weight distribution), we must also expect that the efficiency of fractionation will be

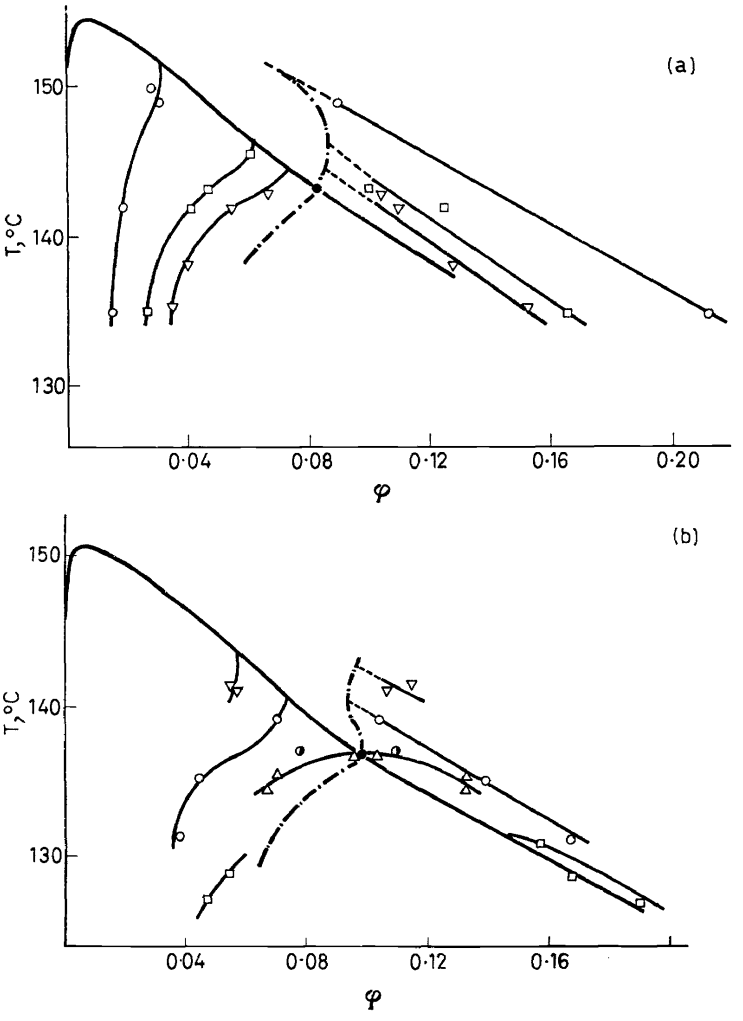

Figure 9. Quasi-binary phase diagrams for two samples of polyethylene dissolved in diphenylether. The characteristics of the samples are given in *Table 2*. Cloud-point curve: ————; coexistence curves for various whole polymer volume fractions: ————; shadow curve: — · — · —; critical point: ●. (a): sample L 30-0-7: $\phi = 0{\cdot}0309$ (○), 0·0612 (□) and 0·0734 (▽). (b): sample L 30-5-1: $\phi = 0{\cdot}0563$ (▽), 0·0733 (○), 0·0854 (◑); 0·0973 (△, critical concentration) and 0·1445 (□).

influenced by the composition of the polymer to be fractionated. Consequently, it cannot be taken for granted that, under otherwise comparable conditions, polymer fractionation will always lead to the same efficiency of fractionation. This is illustrated in *Figure 11* where calculated and measured average molecular weights are compared. Again, we note a high degree of qualitative agreement. Judged by the molecular weight averages, the

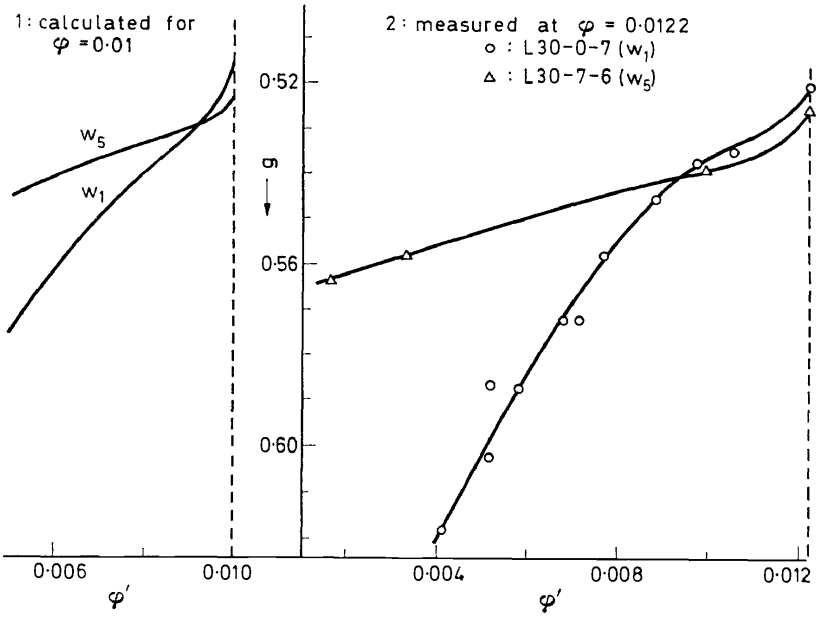

Figure 10. Calculated and measured dilute phase branches of the coexistence curve for relatively narrow (w_5; L 30–7–6) and wide (w_1; L 30–0–7) distributions. Characteristics in *Tables 1* and *2*.

Table 2. Characteristics of polyethylene samples

Sample	$M_n.10^{-3}$	$M_w.10^{-5}$	$M_z.10^{-5}$	M_w/M_n	M_z/M_w
L 30-0-7	12	1·53	9	13	6
L 30-7-6	92	1·4	3·3	1·5	2·4
L 30-5-1	8·6	0·55	3	6·4	5·5

fractionation result at a given fraction size depends to a large extent on the initial polymer distribution.

The characteristics of the hypothetical distributions and those of the Marlex-type polyethylene samples used are collected in *Tables 1* and *2*. The parameter x stands for the mass of the fraction in the polymer-rich phase relative to that of the whole polymer. The g values in the experimental examples (*Figure 10*) have been derived from the $g(T)$ function for the system polyethylene-diphenyl-ether[17,18].

In quasi-binary systems, phase separation must be effected by changing the temperature. This is not the customary approach in which isothermal conditions are maintained and a non-solvent is added. Calculations on quasi-binary systems are however simpler and, moreover, lead to quite analogous conclusions. Some comparisons will be made in Section 3.

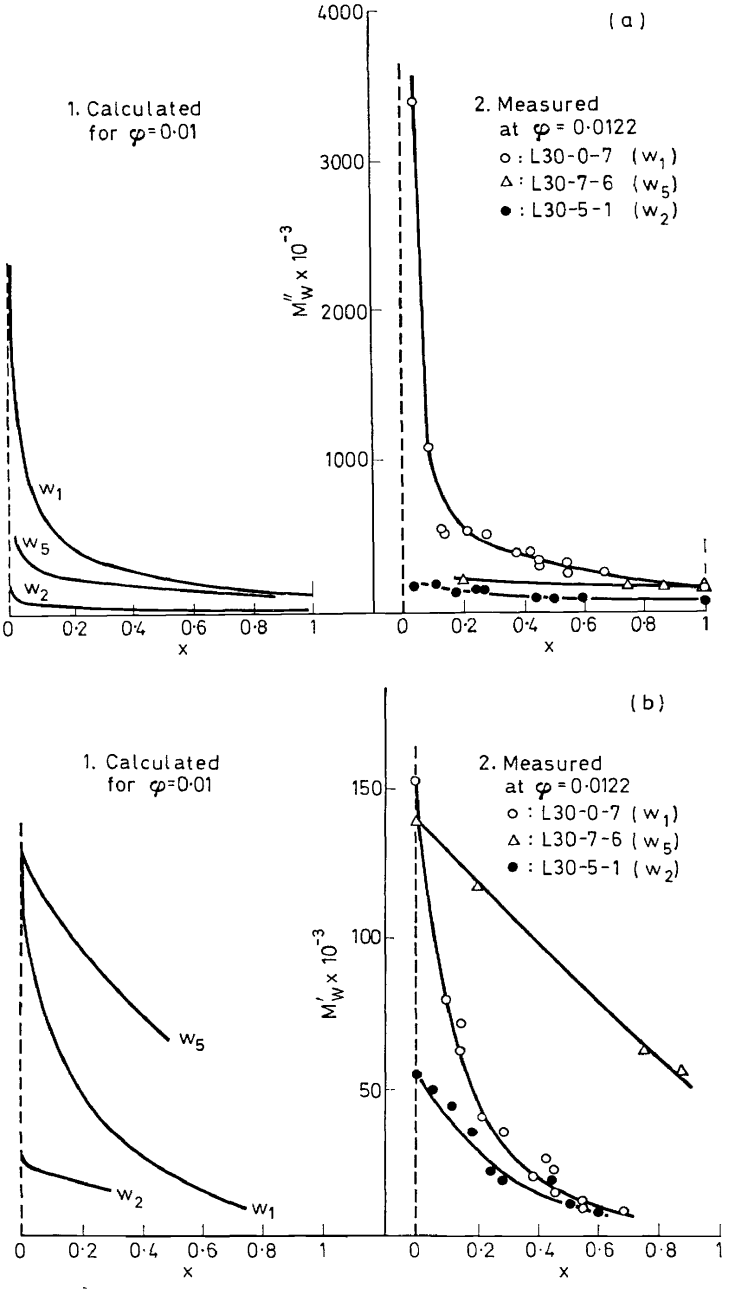

Figure 11 a and *b*. Calculated and measured average molecular weights of the fractions in dilute (single prime) and concentrated (double prime) phases. The abcissa shows the relative size x of the fraction in the concentrated phase.

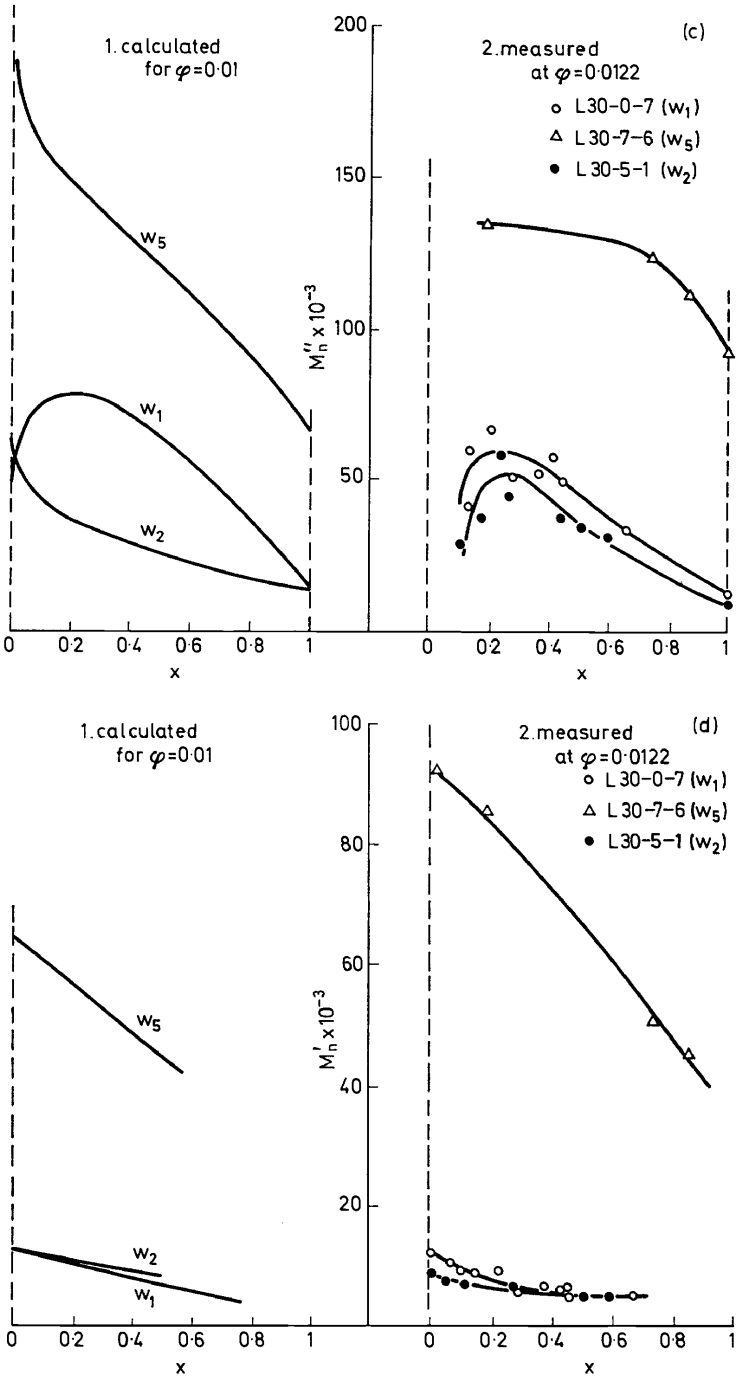

Figure 11 c and *d*.

3. PREPARATIVE FRACTIONATION

a. Precipitation and extraction

It is an established view in fractionation practice that efficient separation is most likely to take place in very dilute solution. A condition is that the dilute phase has a large volume compared with that of the polymer-rich phase[1–3]. This involves the fraction size x being small. Obviously, we refer here to fractional precipitation.

Looking at a ternary diagram, one can easily see that fulfilment of these conditions indeed guarantees the best fraction obtainable in the existing circumstances. Inspection of *Figure 12* discloses that the composition of the

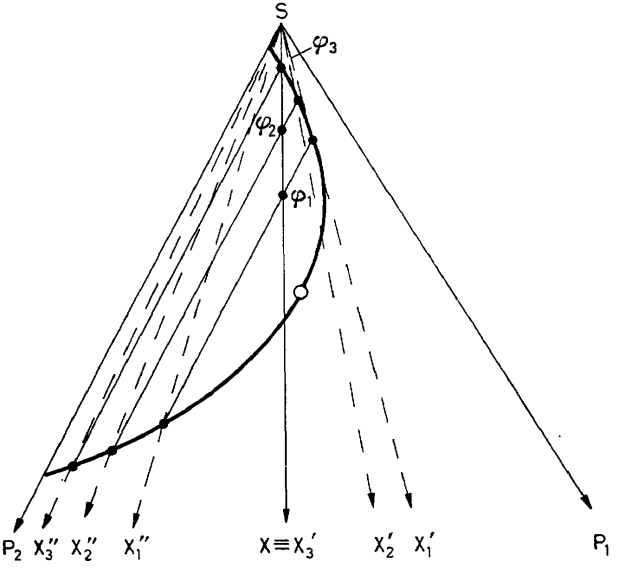

Figure 12. Fractionation of a binary polymer in a quasi-binary system.

fraction in the concentrated phase (X'') shifts towards the pure component P_2 if the overall concentration decreases (X_1'' and X_2'' at ϕ_1 and ϕ_2). At the same time, the ratio V'/V'' of the dilute and concentrated phases rises, and x decreases. The best fraction obtainable at the temperature for which *Figure 12* is valid is X_3''; the corresponding ϕ value is ϕ_3, the threshold concentration. Here, $V'/V'' = \infty$ and $x = 0$.

It is not evident whether or not this simple line of reasoning can be followed also with regard to multicomponent polymer solutions. We shall therefore again refer to numerical calculations and look for the conditions under which a precipitation fraction has the lowest possible M_w/M_n value. The parameters of experimental interest are the overall polymer concentration ϕ and the fraction size x, and it will be interesting to know how M_w/M_n (later referred to by b) for chosen initial distributions depends on x at given ϕ.

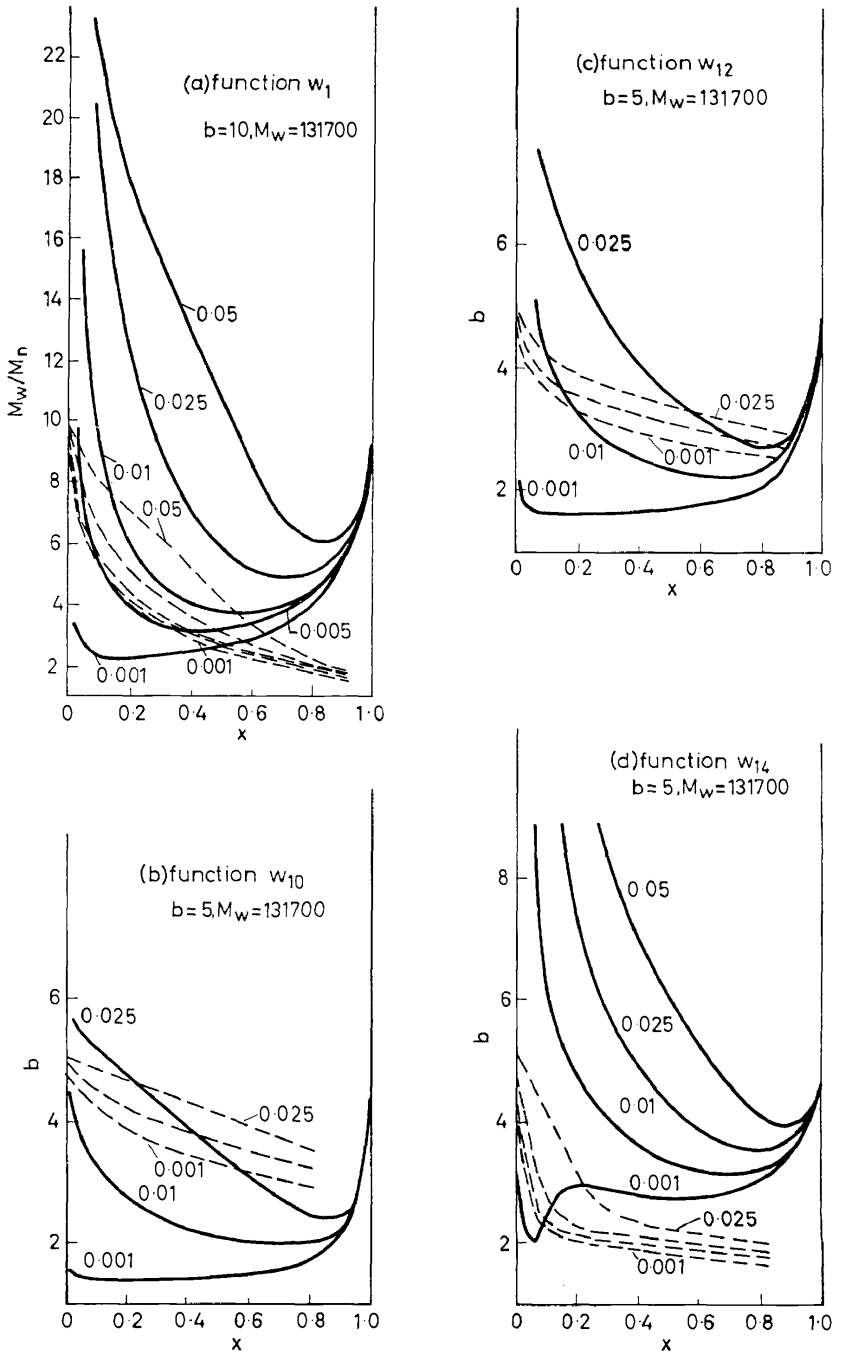

Figure 13. Relation between b-value and relative size x of the fraction for various indicated values of the overall polymer volume fraction ϕ. Drawn curves: fraction in concentrated phase; dashed curves: fraction in dilute phase.

Figure 13 shows this dependence for four different initial distributions and reveals that the fractionation efficiency at given ϕ and x indeed depends on the composition of the original material. The striking feature of the (drawn) $b''(x)$ curves is that, although they do show a minimum, this is not located at $x = 0$. This feature is quite general; it was found for all distribution functions investigated so far[17,18,20,31]. Bohdánecky, who used a different calculation procedure, also points to the occurrence of minima in $b''(x)$ curves[32].

The fractionation rule mentioned above is reflected in the decrease of b'' with ϕ at constant x. However, a decrease of x to the usually recommended low value may lead to a most unwanted result. There exist initial distributions for which this procedure would yield a fraction having a larger b-value than the original material. Both in preparative and analytical fractionation this must be regarded as a most unattractive aspect of the precipitation procedure.

The latter phenomenon can be explained by means of the well-known fractionation equation[9]:

$$w''(M) = w(M)/[1+r \exp(-\sigma m)] \tag{4}$$

where $w''(M)$ = the differential weight distribution of the fraction in the concentrated phase,
$w(M)$ = the differential weight distribution of the initial polymer,
$r = V'/V''$ = the volume ratio of dilute and concentrated phases,
m = the relative chain length of molecules with molecular weight M,
σ = a separation parameter[9], depending on g and on the polymer concentrations in the two phases.

The denominator tends to unity at very high M and is maximum at low M. Hence, if $w(M)$ were constant, $w''(M)$ would decrease with M. If, meanwhile, $w(M)$ should rise steeply, this would offset the decrease of $w''(M)$, and eventually lead to bimodality of $w''(M)$. Anyhow, the asymmetry of $w(M)$ is likely to cause a relative accumulation of low-molecular weight material in $w''(M)$, thereby lowering M_n''. At the high-molecular weight end $w''(M)$ becomes nearly identical to $w(M)$ so that $w(M)$ itself determines M_w'' to a high degree. This accounts for the high value of b'' $(= M_w''/M_n'')$, which in some cases may even exceed b.

Figure 13 also suggests a method of fractionation that seems to hold out much greater promise. At high x values all $b'(x)$ curves (denoting the b value of the dilute-phase fraction as a function of x) drop to relatively low values. This phenomenon is not so common as the minimum in $b''(x)$, and the sharpening of the fraction distribution depends to a large extent on the initial distribution[17,18,20,31]. This can be seen from the curve for function w_{10} in *Figure 13*. However, the $b'(x)$ function shows little dependence on the polymer concentration and this means a considerable advantage in large-scale preparative fractionation. Whereas in fractional precipitation the concentration must be kept low, this variant of fractionation by extraction allows it to be taken as high as handling of the solution allows. Then, large amounts of initial material can be manipulated without the need for exces-

sive solution volumes. In fact, the polyethylene samples L30-7-6 and L30-5-1 (*Table 2*) were prepared in this way, starting from 1 kg of sample L30-0-7.

Scott[33] already noted that extraction might yield more favourable results than precipitation. However, in normal extraction procedures, in which the bulk polymer is successively extracted with liquids of increasing solvent power, equilibrium can hardly be established. This tends to broaden the

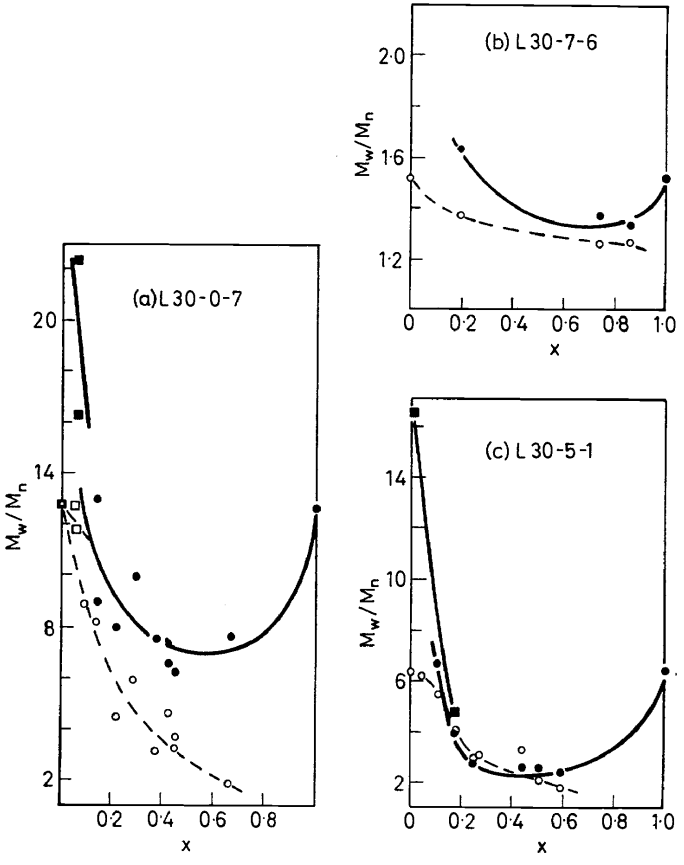

Figure 14. Width of the fraction distribution as a function of the fraction size x. Circles and squares denote 1 per cent and 2 per cent initial polymer concentrations, respectively. Closed symbols: concentrated phase; open symbols: dilute phase. Polymer samples: Marlex-type polyethylene (see *Table 2*); solvent: diphenylether.

fraction distributions. To overcome this practical drawback, Staverman and Overbeek[34] suggested the precipitation of most of the polymer as a concentrated phase, and the isolation of the material remaining in solution. This variant of the extraction method is actually the procedure discussed above.

The effects described so far can be verified experimentally[17,18], as is shown in *Figure 14*.

b. Influence of the free enthalpy of mixing function

All preceding considerations were derived from calculations based on Eq. (2), with g independent of ϕ. Before formulating a general conclusion about preparative fractionation, we shall first investigate the effect of ΔG functions deviating from Eq. (2) which has been used so far. There may be two causes of such deviations:

(i) in quasi-binary systems g is generally found to depend on ϕ;

(ii) most fractionations reported in literature were not carried out in quasi-binary, but in quasi-ternary solutions, which consist of a solvent, a precipitant and the polymer.

(*i*) *Concentration-dependent interaction parameter*

The numerical fractionation calculations can be readily carried out with a concentration-dependent g. We did not normally adopt this procedure

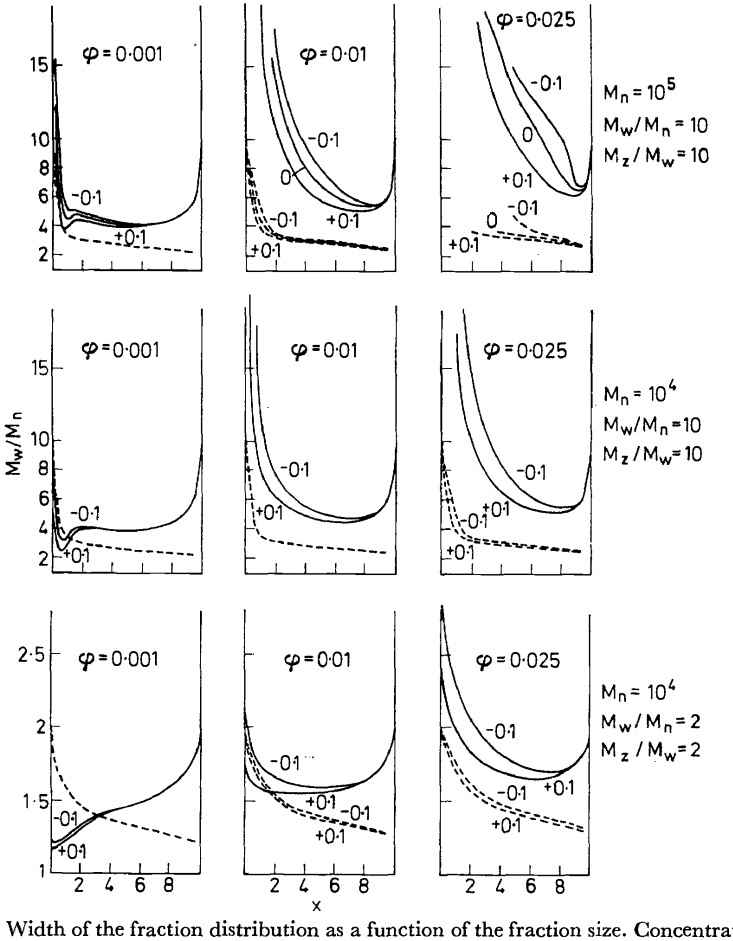

Figure 15. Width of the fraction distribution as a function of the fraction size. Concentration-dependent interaction parameter, values of g_1 ($= \partial g/\partial\phi$) are indicated. Fraction in concentrated phase: ————; in dilute phase: — — — —. Initial distributions: sums of two exponential functions.

because the choice of the $g(\phi)$ function involves a certain arbitrariness. For the present purpose we chose g linearly dependent on ϕ:

$$g = g_0 + g_1\phi \tag{5}$$

and restricted the $g(T)$ function to g_0.

The $b(x)$ graphs for two values of g_1 are shown in *Figure 15*, which demonstrates that the overall picture is preserved but for a shift of the curves. With $g_1 > 0$, we get a better fractionation efficiency than with $g_1 = 0$. A negative value of g_1 has an unfavourable effect.

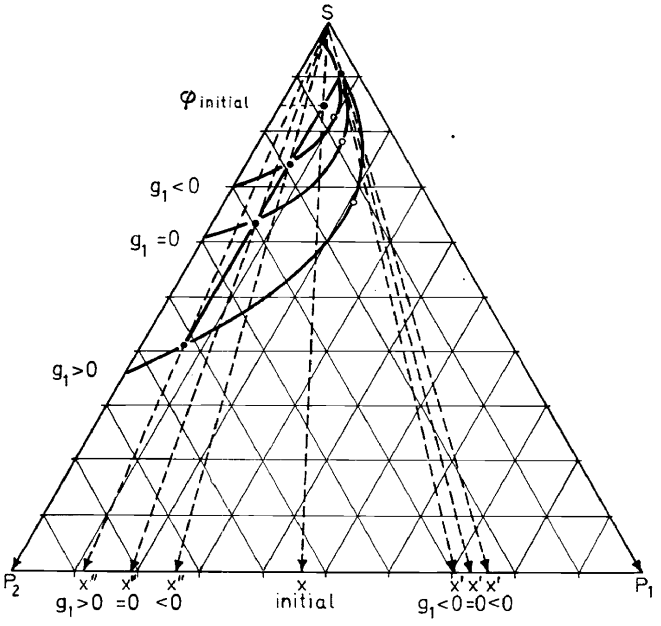

Figure 16. Fractionation at varying concentration dependence of the interaction parameter g ($g = g_0 + g_1\phi$).

This can be understood by looking at a ternary diagram (*Figure 16*). Under comparable conditions (such values of g_0 that we have equal ϕ and equal x) we get a wider miscibility gap with $g_1 > 0$ than with $g_1 = 0$, and a narrower one with $g_1 < 0$. This means that the fraction in the concentrated phase X″ will be nearest to the pure component P_2 if $g_1 > 0$. *Figure 16* suggests that a negative g_1 also has an unfavourable effect on the width of the fraction in the dilute phase. This is in agreement with *Figure 15*.

However, we have seen that not too much significance should be attached to these ternary graphs; therefore the conclusions drawn from them should be verified against truly multicomponent solutions. This has been done in *Figure 17*, which shows the relative location of some coexistence curves if g depends on ϕ. The immiscibility region is widest with $g_1 > 0$.

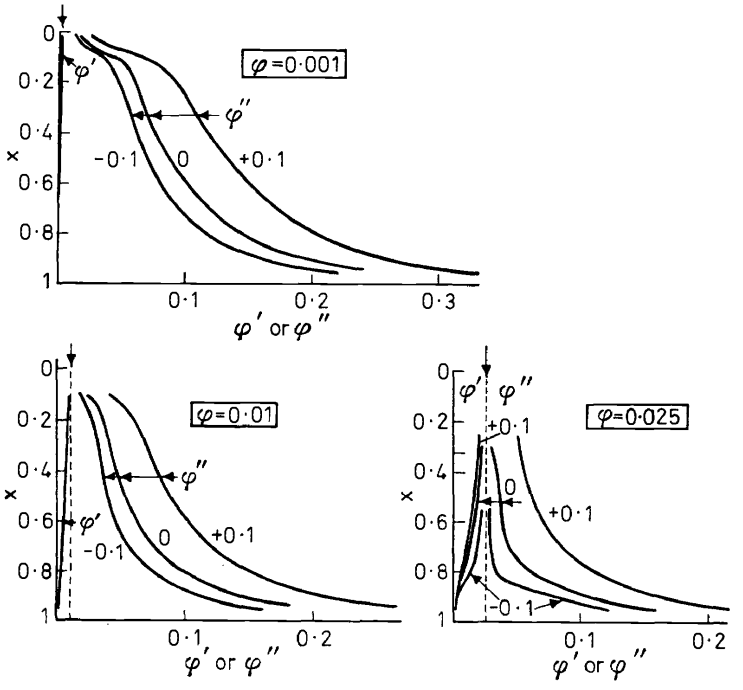

Figure 17. Coexisting phase concentrations ϕ' and ϕ'' at various indicated values of g_1 ($g = g_0 + g_1\phi$) and various overall polymer concentrations ϕ. Initial distribution: sum of two exponential functions; $M_n = 10^5$; $M_w/M_n = 10$; $M_z/M_w = 10$.

(ii) Solvent–non-solvent–polymer

Calculation of phase equilibria in quasi-ternary solutions calls for a ΔG function which is more complicated than Eq. (2). Now allowance must be made at least for the three binary interactions, which can be done by extending Eq. (2)[7,9]. If we assume that both the solvent and the non-solvent molecules have the size of a lattice site, we get:

$$\Delta G/RT = \phi_0 \ln \phi_0 + \Sigma \phi_i m_i^{-1} \ln \phi_i + \psi \ln \psi + g_{01}\phi_0\phi + g_{02}\phi_0\psi + g_{12}\phi\psi \quad (6)$$

where ψ is the volume fraction of the non-solvent and g_{01}, g_{02} and g_{12} denote the solvent–polymer, solvent–non-solvent and non-solvent–polymer interaction parameters, respectively.

Many combinations of the g values are conceivable. For the moment, we shall consider only one set of values to form an idea as to whether the overall shape of the $b(x)$ curves derived so far is valid also in the case of precipitation by a non-solvent. *Figure 18* demonstrates that this question can be answered in the affirmative. The set of g values used for calculating the quasi-ternary $b(x)$ curves is: $g_{01} = 0$; $g_{02} = 0$; $g_{12} = 1$. This set represents a very good solvent for the polymer and a readily miscible solvent–non-solvent pair.

As can be seen in *Figures 15* and *18*, the behaviour revealed by *Figure 13*

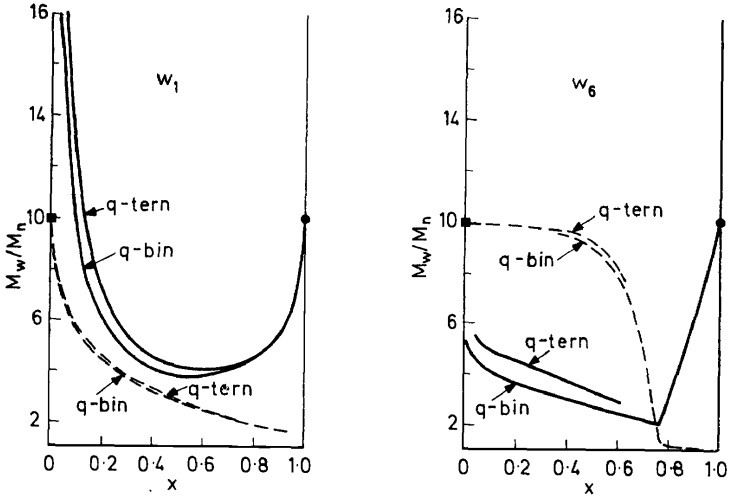

Figure 18. Comparison of the fractionation efficiency in quasi-binary (poor solvent-polymer) and quasi-ternary (solvent–precipitant–polymer) systems. Values of the interaction parameters: $g_{01} = 0$, $g_{02} = 0$, $g_{12} = 1$. Overall polymer volume fraction: 0·01. Fraction in concentrated phase: ————; in dilute phase: — — — —.

can be regarded as quite general, whatever the nature of the system in which the fractionation takes place.

c. Influence of initial distribution

In the preceding examples the initial distributions, whether unimodal or showing two maxima, invariably have a positive skewness. Although one would intuitively expect polymer distributions to have such shapes, it is nevertheless instructive to examine what might be the effect of other shapes on the fractionation efficiency.

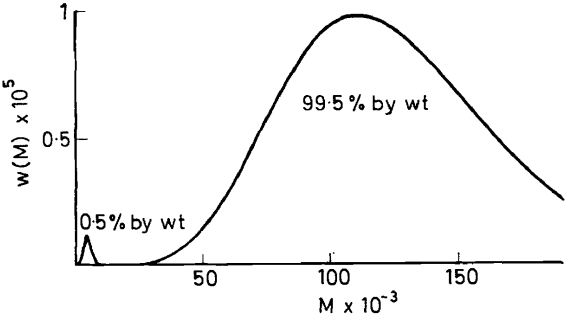

Figure 19. Narrow distribution (main peak w_{15}; $M_w = 1{\cdot}256 \times 10^5$, $b = 1{\cdot}13$), contaminated with a small amount of low molecular weight material (total two-peaked distribution; w_{16}; $M_w = 1{\cdot}250 \times 10^5$; b = 1·25).

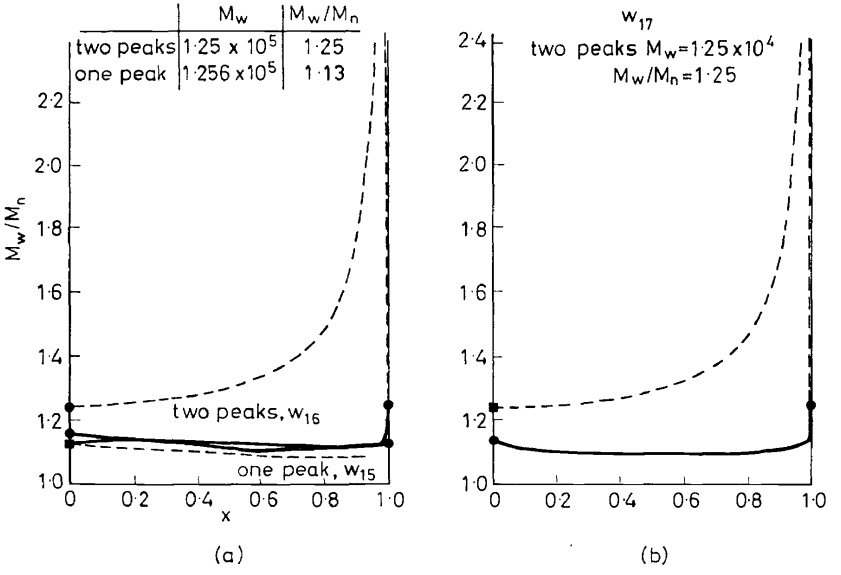

Figure 20. Fractionation efficiency with the contaminated distribution in *Figure 19.* Fraction in concentrated phase: ————; in dilute phase: — — — —; $\phi = 0{\cdot}01$.

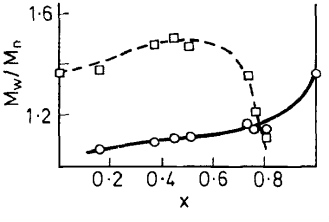

Molecular weight distribution of the initial polystyrene sample
(G P C analysis)

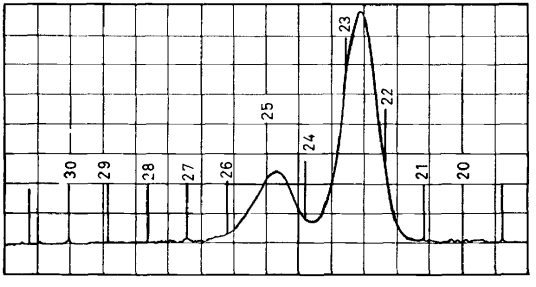

Figure 21. Fractionation efficiency for a mixture of two narrow-distribution polystyrene samples. Initial concentration: 1 per cent by weight; solvent: cyclohexane. Fraction in concentrated phase: ————; in dilute phase: — — — —.

As a first example let us consider a narrow distribution contaminated with a small amount of low-molecular weight polymer (*Figure 19*). The corresponding $b(x)$ curves are illustrated in *Figure 20*, which shows a behaviour rather different from that observed before. Over practically the whole x range, the fraction in the dilute phase now has a wider distribution than the original polymer.

For the explanation we again refer to Eq. (4). As long as x is smaller than 0·995, the dilute phase will contain contributions from both peaks. This gives rise to relatively large b' values which will increase with x. When the x value of 0·995 is exceeded the dilute phase will finally contain only

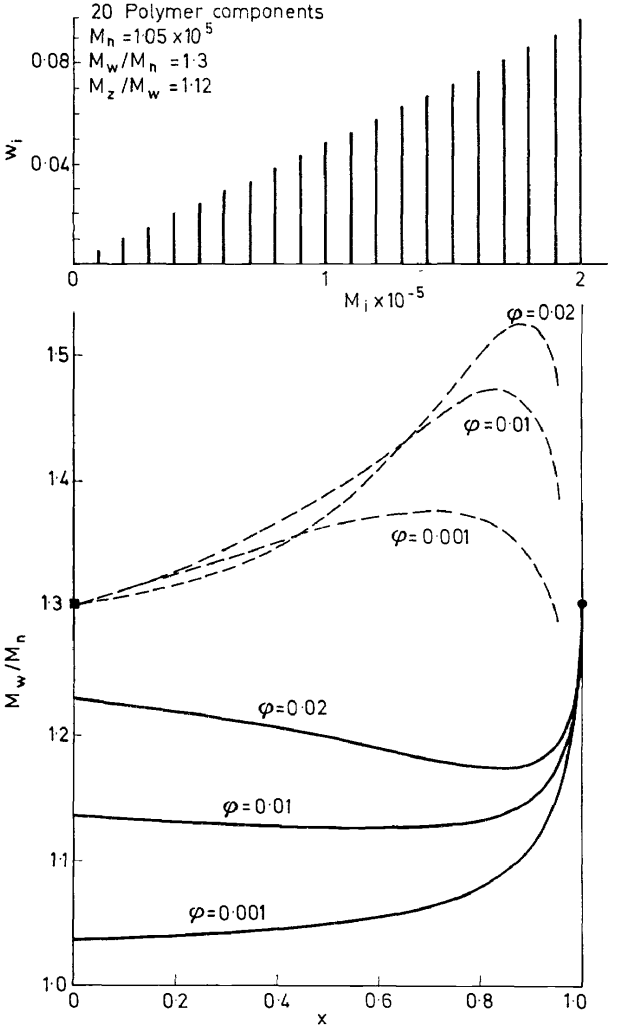

Figure 22. Fractionation efficiency for a negatively skewed initial distribution. Fraction in concentrated phase: ————; in dilute phase: — — — —.

constituents from the low-peak material and, consequently, b' must drop sharply. At a lower molecular weight level, we observe the same phenomenon (*Figure 20b*).

Although, strictly speaking, the Staverman-Overbeek extraction method would still yield a good fraction, this will in the present case only be so at impractically high values of x. Indiscriminate application of the Staverman–Overbeek extraction procedure would then have an undesired effect, in that it would lead to a fraction having a wider distribution than the initial polymer.

This conclusion needs experimental verification, which is supplied by *Figure 21*. The effect, although clearly visible, is less pronounced than in the calculated examples because the two peaks are closer together and do not differ so much in magnitude.

The second example is a logical continuation of the preceding one. We now consider an initial distribution with a negative skewness. Kubín developed a very useful continuous distribution function which covers this case[35]. His function is a generalized exponential distribution having three adjustable parameters, one of which is a power exponent of M in the exponential. Unfortunately, this function cannot be introduced into our current computer programme, and we used the, admittedly crude, approximation of a set of δ functions.

Figure 22 demonstrates that, in this case, the behaviour is identical with that for the previous, contaminated distribution and here also Staverman–Overbeek extraction, if used indiscriminately, leads to undesired results.

d. Preparation of fractions

The material assembled indicates that the fractionation efficiency depends greatly on the initial distribution. Since the latter is not as a rule known, we must look for a phenomenon appearing at all polymer compositions and concentrations. Inspection of the data reveals that the width of the fraction in the concentrated phase at large values of x is such a general characteristic. We always note a sharp drop of the $b''(x)$ curve in that region of x values. Hence, the safest procedure in the preparation of fractions from, *a priori*, unknown distributions would seem to be repeated extraction of the concentrated phase at high x values. If the initial distribution has a positive skewness, we can just as well use the extracted material (Staverman–Overbeek extraction); if it has not, the extracted fractions will be useless.

This procedure of repeated extraction, which can be applied to solutions of comparatively high concentrations, will, by its very nature and also because of the large x values involved, be highly suitable for large-scale use. There is a limit to its applicability, however, because the drop of $b''(x)$ at high x values decreases with the width of the original distribution. *Figure 23* illustrates this rather obvious effect. If b decreases, the $b''(x)$ curves tend to level out and, below $b = 1{\cdot}1$, the effect of further extractions cannot be expected to be anything but small. Beyond this point we depend on other methods.

If the polymer is capable of crystallizing, fractional crystallization would be a powerful means of obtaining sharper distributions[36–38]. For non-crystallisable polymers we have to rely on other means. A possible solution

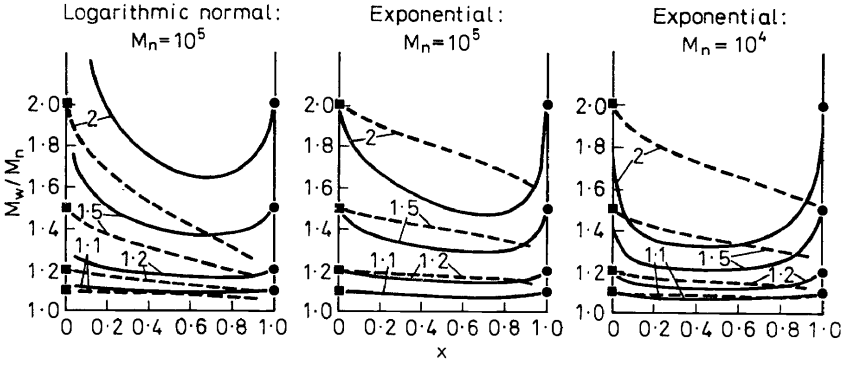

Figure 23. Influence of the width of the initial distribution (b-values are indicated) on the efficiency of fractionation at $\phi = 0{\cdot}01$. Fraction in concentrated phase: ————; in dilute phase: — — — —.

is offered by the counter-current extraction technique proposed by Englert and Tompa[39].

It might also be possible to conclude the repeated extraction by removing the high molecular weight tail as a result of a precipitation step at low x. If, however, in the course of the extraction process a negatively skewed distribution has developed in the product, such a final step would only have an undesired effect. *Figure 22* illustrates this, since at low x we have $b' > b$. Occurrence of a negatively skewed distribution during repeated extraction is by no means improbable, as is schematically shown in *Figure 24*.

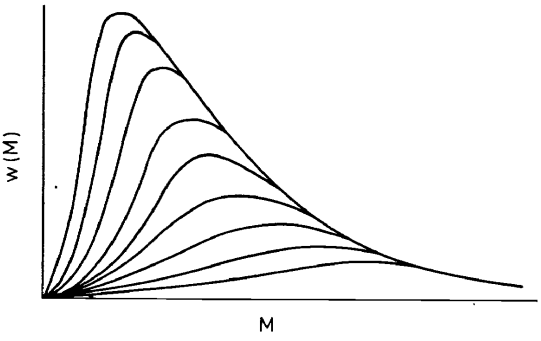

Figure 24. Possible course of repeated extraction of a positively skewed initial distribution.

4. THE ANALYTICAL PROBLEM

a. Analysis of fractionation data

In attempts to determine the molecular weight distribution, the polymer may be separated into a number of fractions. For this purpose several fractionation schemes have been devised[1–5], all of which share the difficulty that the initial distribution must be reconstructed from the data available.

We shall not go into a detailed discussion of the various schemes and evaluation methods[17,18,25,40], but restrict ourselves to giving some representative examples.

One possible way of accounting for the distribution present in every fraction is by making use of functions like Eqs. (1) and (3). The distribution parameters appropriate for each fraction are calculated from its average molecular weights, M_n or M_w or both, as in the case of exponential and logarithmic normal functions. Having done this for all fractions, the individual functions can be added. This yields curves, which may be considered representative of the initial polymer.

In theoretical fractionation where the initial distribution is known, we

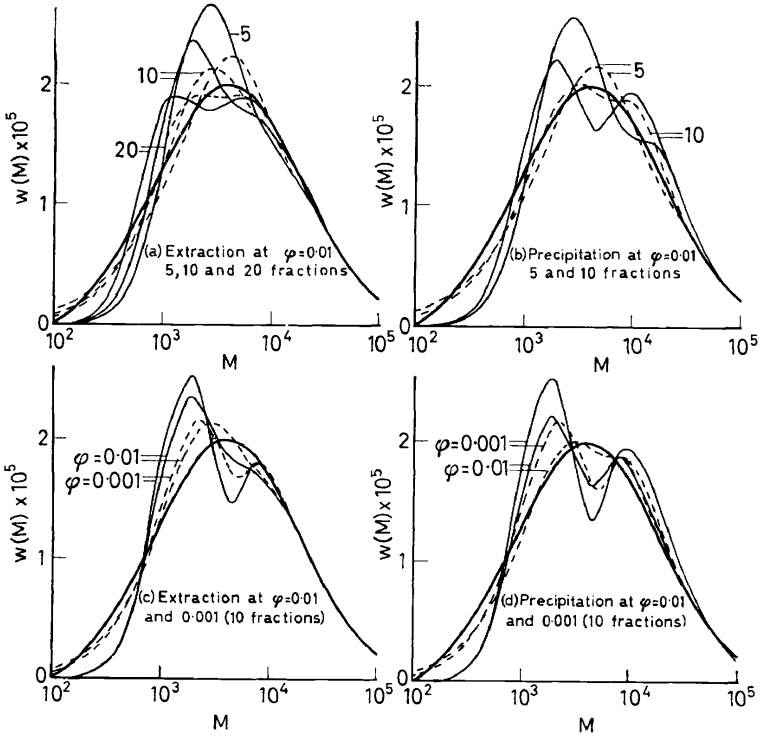

Figure 25. Successive fractionations of function w_1 (————). Logarithmic normal and exponential fraction distributions: ———— and — — — —.

can check the resulting curves against the original function chosen. Compared with the experimental approach, where such a comparison can be made in rare cases only, this gives a distinct advantage.

Figures 25 and *26* show the results of calculated fractionations of the initial distributions w_1 and w_6 (*Table 1*). These refer to fractionation by successive extraction and precipitation of various numbers of fractions at two different concentrations. It can be seen from these figures that an

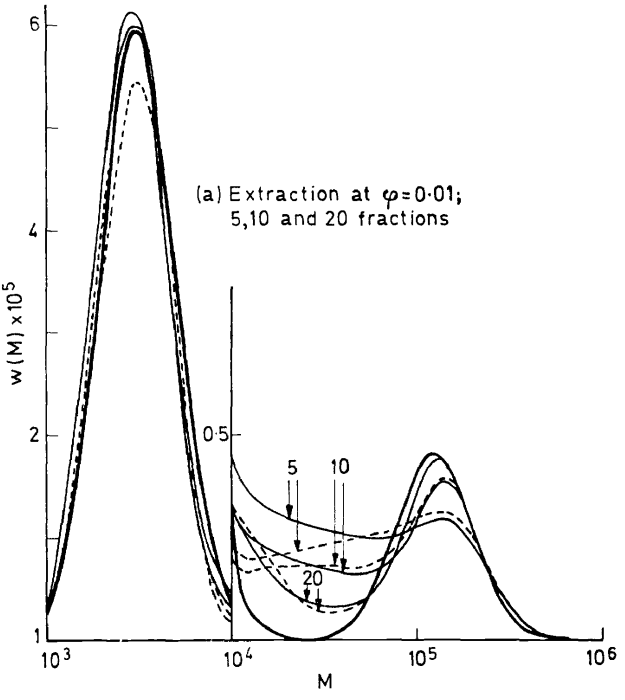
(a) Extraction at φ=0·01;
5,10 and 20 fractions
w(M) x10^5
M
5
10
20
0·5
1
2
4
6
10^3
10^4
10^5
10^6

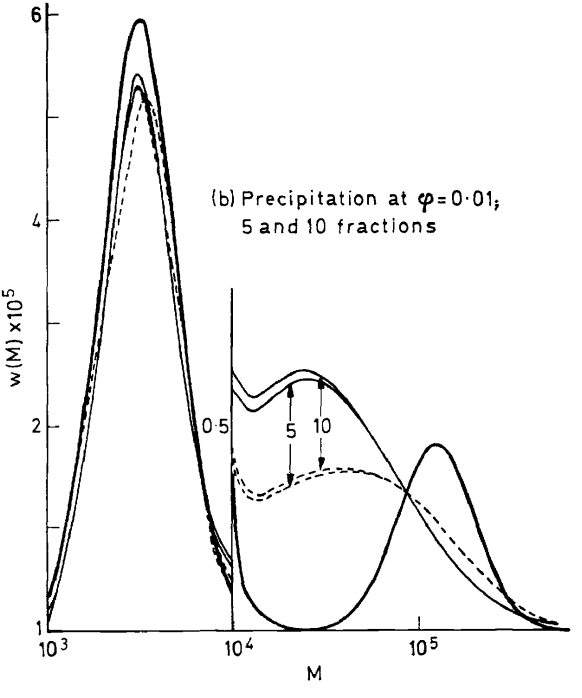
(b) Precipitation at φ=0·01;
5 and 10 fractions
w(M) x10^5
M
5
10
0·5
1
2
4
6
10^3
10^4
10^5

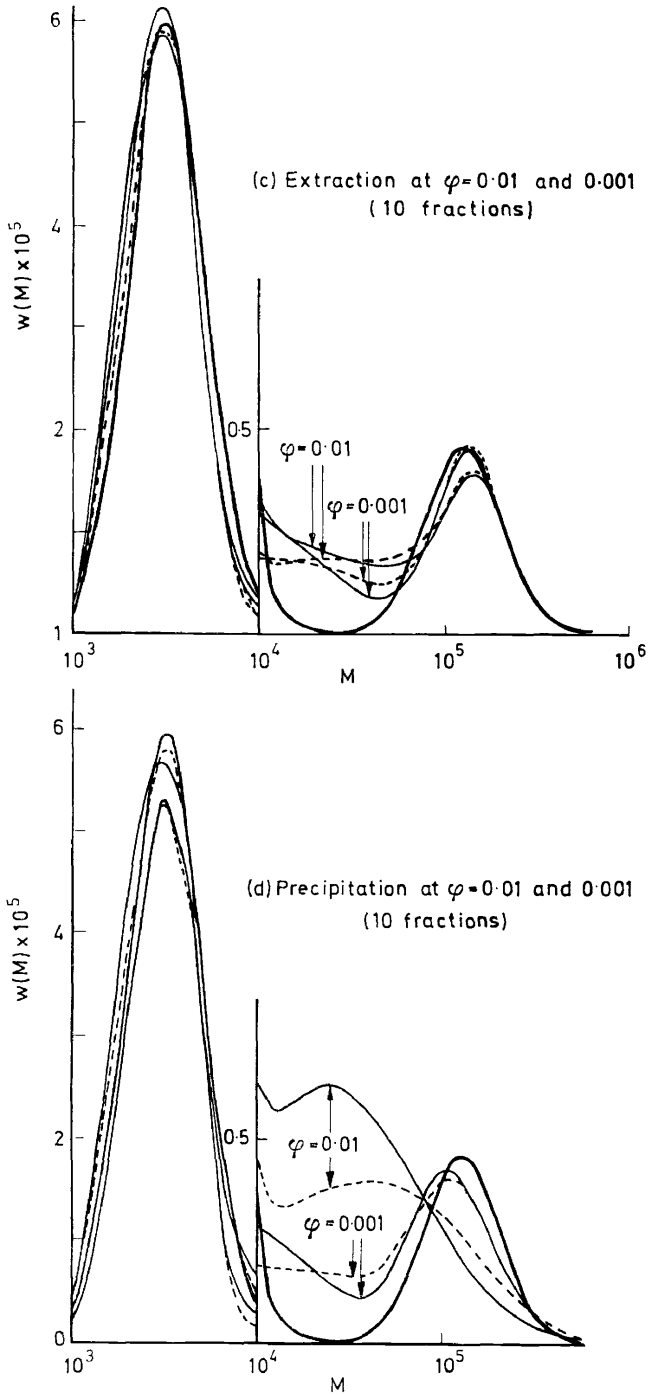

Figure 26. Successive fractionations of function w_6 (————). Logarithmic normal and exponential fraction distributions: ———— and — — — —.

accurate approximation of the original distribution cannot easily be obtained by fractionation. This is due to insufficient correspondence between actual fraction distributions and their representations[17,18]. A drawback of the evaluation method used here is that extra peaks may be introduced, which are not present in the original curve, whereas, on the other hand some secondary peaks may be overlooked. Hence, reliable detailed information cannot be derived from fractionation methods. The only procedure which appears to lead to a meaningful result is successive extraction into a large number of fractions.

These conclusions refer to calculated examples in which experimental errors do not play a rôle. In addition to the considerable experimental effort involved in a multi-step extraction, there is the notorious loss of material during fractionation, which detracts from the reliability of the result. In view of all this, it seems questionable whether the unreliable results will ever justify the efforts devoted to analytical fractionation.

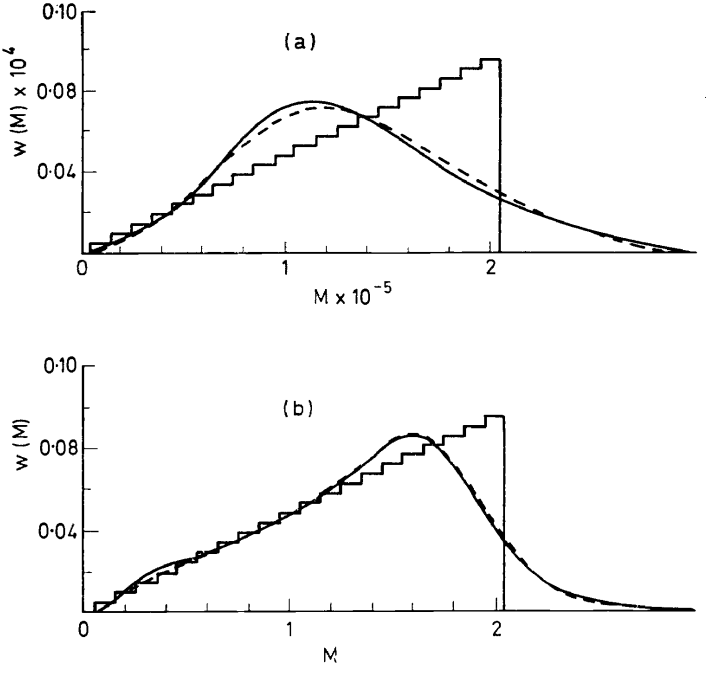

Figure 27. Successive fractionations into 10 fractions of a negatively skewed distribution ($\phi = 0{\cdot}01$). Logarithmic normal and exponential fraction distributions: ——— and — — — —. *a*: precipitation; *b*: extraction.

A further example is shown in *Figure 27*, where the negatively skewed set of δ functions (see *Figure 22*) is represented by a step curve, to facilitate comparison with the results of the fraction data analysis. With successive precipitation, the negative skewness disappears altogether. Admittedly, the representation of the fraction distributions by positively skewed functions

[(1) and (3)] cannot but be rather inappropriate, but given the present result, there is no way of knowing this.

It is generally believed that fractionation, whether preparative or analytical, should be carried out in dilute solution. We have seen, however, that extraction at relatively high concentrations may yield quite satisfactory fractions. It has been shown elsewhere[17,18,41] that this holds even at concentrations higher than the critical. *Figure 28* shows an example of the

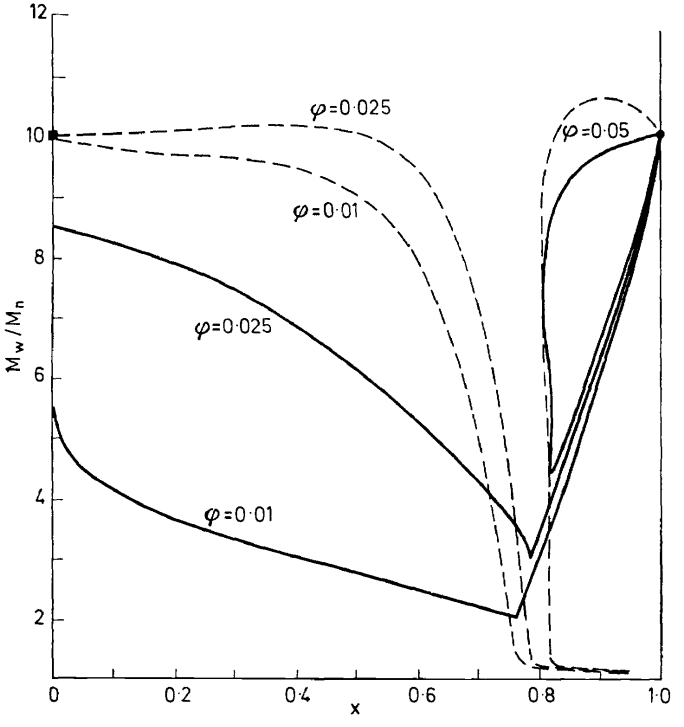

Figure 28. Fractionation efficiency for bimodal distribution w_6. Fraction in concentrated phase: ————; in dilute phase: — — — —.

bimodal distribution w_6 (*Table 1*, *Figure 7*). At $\phi = 0{\cdot}05$ ($\phi_c = 0{\cdot}03571$), the $b'(x)$ curve shows a branch tending down to relatively small b' values. Complete fractionation by extraction under these conditions yields the result shown in *Figure 29*. The reconstruction of w_6 is not very satisfactory, though not much worse than some of the examples in *Figure 26*. A better result is obtained with function w_1 (*Figure 29*), and the narrower initial distributions w_5 and w_7 can be quite reasonably reconstructed (*Figure 30*).

b. Alternative approach

In Section 1 arguments were advanced suggesting that liquid–liquid phase relationships are to a large extent determined by the molecular weight distribution. Should this be so, the question arises whether phase relations

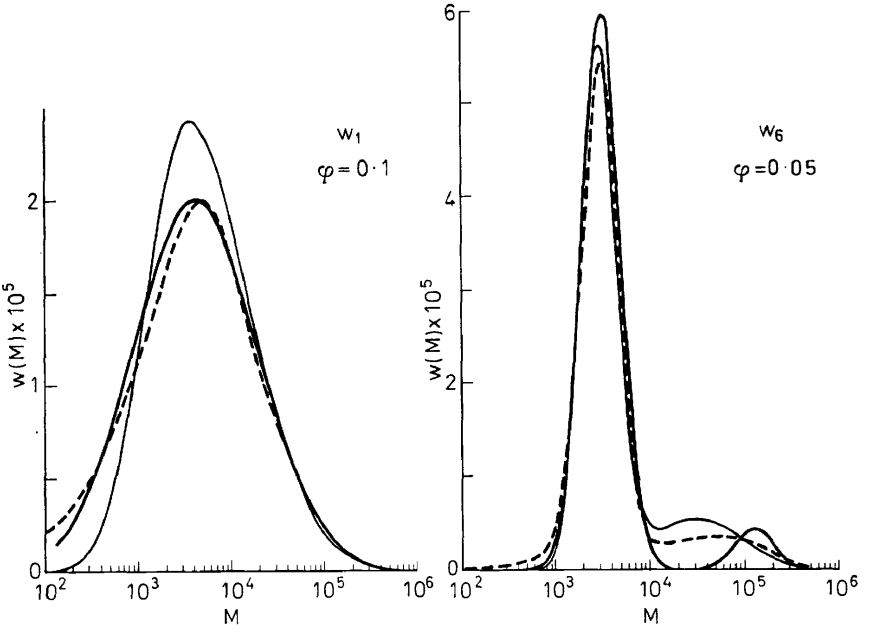

Figure 29. Supercritical successive extraction of functions w_1 and w_6 (————). Logarithmic normal and exponential fraction distributions: ———— and — — — —.

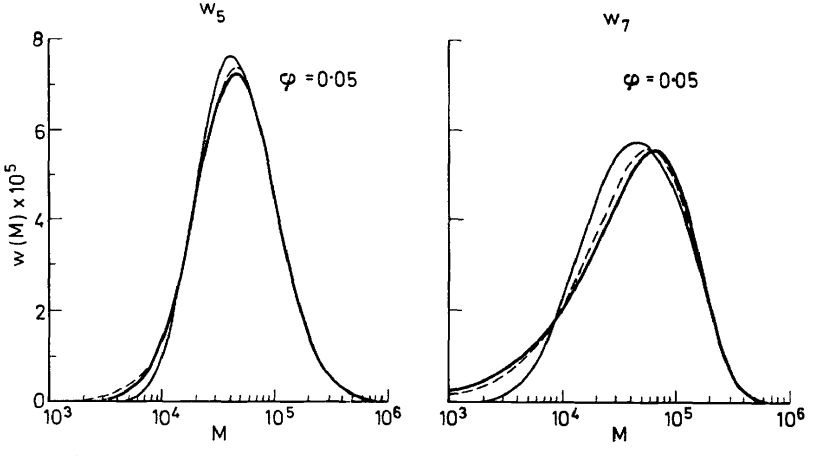

Figure 30. Supercritical successive extraction of functions w_5 and w_7 (————). Logarithmic normal and exponential fraction distributions: ———— and — — — —.

might not be employed for estimating the polymer composition. The situation for a binary polymer is sketched in *Figure 31.* Evidently, if the location of the binodal were exactly known, a single phase-volume-ratio determination at a given value of ϕ would suffice for establishing the position of X.

Attempts to extend this principle to multicomponent systems have met with considerable difficulties[7,8,42]. These are threefold in nature. In the first place, the location of the binodal must be known with great precision. This calls for very accurate knowledge of the ΔG function. Secondly, the choice of the molecular weights of the polymer components includes a certain arbitrariness. This could probably best be eliminated by introducing a continuous distribution in the form of the sum of several exponential

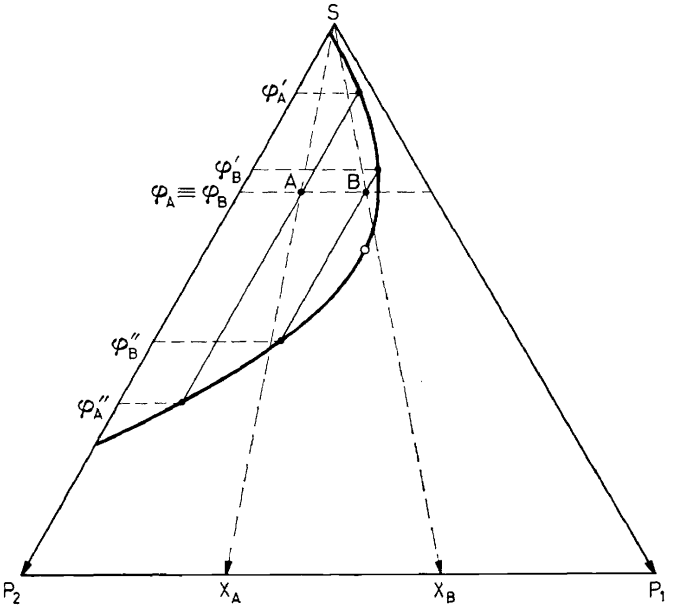

Figure 31. Determination of the composition X of a binary polymer from phase relationships.

functions. Finally, the choice of the number and the accuracy of the experimental data also present problems. Since the original appearance of this method[17,18], progress has been very slow, and only one example has been encountered in which the distribution showed some likeness to that determined independently by means of the ultracentrifuge. The phase relationships used were likewise established with the aid of the ultracentrifuge[43]. *Figure 32* shows the distributions which cover the same molecular weight range and exhibit some similarity in shape.

However, this single example must be regarded as highly fortuitous, and much further work remains to be done in the field. Whatever the outcome, this thermodynamic method will, at any rate, remain very laborious and unsuited for routine measurements. For calibration purposes it might find a useful place among other techniques.

Even if we drop the detailed analysis described above, phase relations will at least give some qualitative insight into the degree of polydispersity.

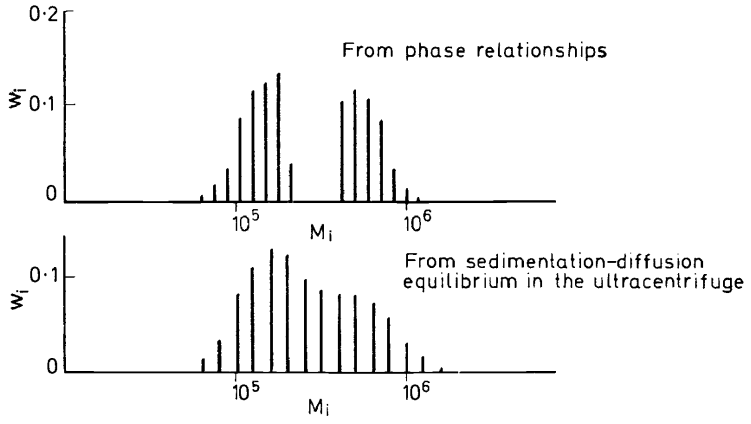

Figure 32. Molecular weight distribution curves for a sample of polystyrene.

Rehage and Wefers[44] presented an interesting example of this behaviour. They determined the cloud-point curve for a sample of narrow-distribution polystyrene in cyclohexane, and found that the precipitation threshold and the critical point were located at concentrations lying a factor 2·4 apart (*Figure 33*). Nevertheless, the sample had a low b value (1·07). Hence, one would expect the distribution to be narrow and, consequently, the threshold and consolute concentrations to be closer together. Determination of the M_z value disclosed the origin of the supposed discrepancy; the ratio M_z/M_w was considerable. This example illustrates that the M_w/M_n value alone is a

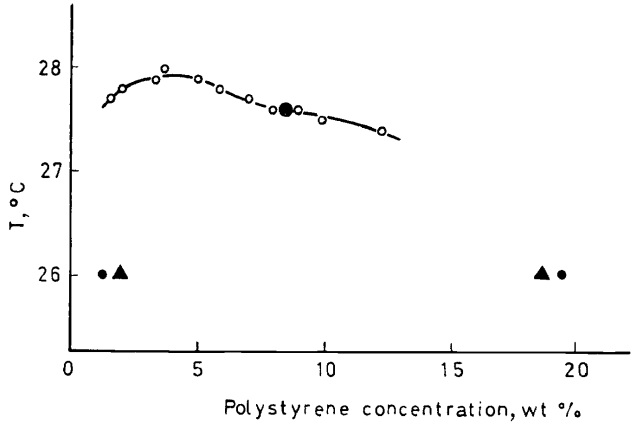

Figure 33. Cloud-point curve of a sample of polystyrene in cyclohexane. Data from Rehage and Wefers[44]. Cloud points: 0, critical point: ⊙; coexisting phase compositions at 2 (●) and 10 (▲) per cent whole polymer concentration. Characteristics of polystyrene sample: $M_n = (4{\cdot}4 \pm 0{\cdot}2) \times 10^5$; $M_w = (4{\cdot}7 \pm 0{\cdot}2) \times 10^5$; $M_z = 6{\cdot}5 \times 10^5$; $b = 1{\cdot}07 \pm 0{\cdot}07$; $M_z/M_w = 1{\cdot}4$.

very ambiguous measure of the polydispersity[17,20] and additional data are needed for obtaining sufficient certainty. One of these might be the M_z/M_w ratio, and another, less direct one, might be the difference in threshold and critical concentrations. When the latter is chosen, it is useful to look for polymer-solvent systems in which g is strongly dependent on the concentration ($\partial g/\partial\phi > 0$), since, as we have seen, this tends to widen the miscibility gap[45].

McIntyre *et al.*[46] also noted that the relation between threshold and critical concentrations reflects the polydispersity of the sample. They proposed to use the ratio ϕ_c/ϕ_{thr} (polymer volume fractions at critical point and threshold) for determining M_w/M_n. Such a relation is not independent of the type of distribution, as is witnessed by *Figure 34*, which shows calculated

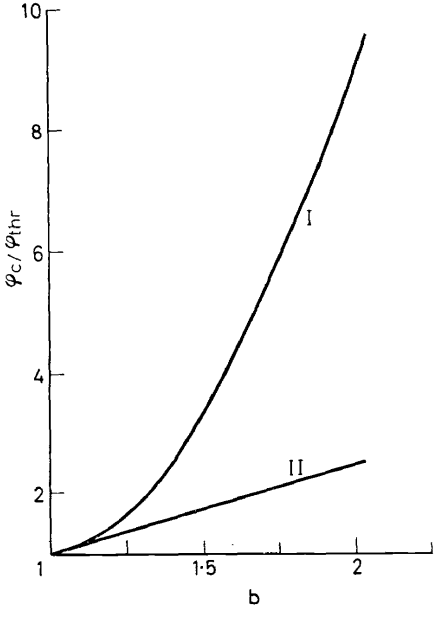

Figure 34. McIntyre plot for logarithmic normal (I) and exponential (II) distributions.

ϕ_c/ϕ_{thr} values for logarithmic normal and exponential distributions. *Figure 34* suggests that the influence of the distribution ceases to exist at low values of b. This is not so much a disadvantage as it may seem, because the method may still serve a useful purpose in the range of very small b values, which cannot be determined with great accuracy by direct measurement of M_n and M_w.

5. CONCLUSIONS

Preparation of fractions with narrow distributions, in particular if carried out on a large scale, is a possible, though laborious procedure. Repeated extraction presents itself as the most reliable method since it is the least

liable to be influenced by the initial distribution and the polymer concentration. The latter aspect makes extraction most suited for scaling-up.

None of the preparative methods considered here comes anywhere near to its ultimate aim, isolation of pure components. It should be realized that, with M_w/M_n values as low as e.g. 1·03, which may rightly be considered a notable achievement, we still (*a*) have an abundant number of components (order of 1000) and (*b*) may, at the same time, find ourselves up against a much higher value of M_z/M_w.

Fractionation does not appear to be a promising means of determining molecular weight distributions with great accuracy. One might consider the possibility of deriving the molecular weight distribution from its influence on phase relationships. A method based on this principle is still in the initial stages of development.

LIST OF SYMBOLS

b = M_w/M_n value of the whole polymer
b' = M_w/M_n value of the fraction
b'' = M_w/M_n value of the fraction
ΔG = free enthalpy (Gibbs free energy) of mixing
g = interaction parameter
M = molecular weight
M_n = number-average molecular weight
M_w = weight-average molecular weight
M_z = z-average molecular weight
m = relative chain length
R = gas constant
r = V'/V''
T = absolute temperature
V', V'' = volumes of the dilute and concentrated phases
W = total mass of polymer
$w(M)$ = differential weight distribution
x = size of the fraction in the concentrated phase, relative to the mass of whole polymer
ϕ_0 = volume fraction of solvent
ϕ_i = volume fraction of polymer species i
$\phi = \Sigma\phi_i$ = whole polymer volume fraction

Acknowledgement

The author is indebted to Dr A. J. Pennings (DSM) for stimulating discussions, and to Prof. G. Rehage (TH, Clausthal-Zellerfeld) for putting *Figure 33* at his disposal.

References

[1] G. V. Schulz. In H. A. Stuart (Ed.) *Die Physik der Hochpolymeren*, Springer Verlag, Vol. II, 1953, p. 726.
[2] L. H. Cragg and H. Hammerslag. *Chem. Revs.* **39**, 79 (1946).
[3] V. Desreux and A. Oth. *Chem. Weekblad* **48**, 247 (1952).
[4] G. M. Guzmán. In J. C. Robb and F. W. Peaker (Eds.) *Progress in High Polymers*, Heywood & Co., London, Vol. I, 1961, p. 113.
[5] M. J. R. Cantow (Ed.) *Polymer Fractionation*, Academic Press, New York, 1967.

[6] L. H. Tung. In D. McIntyre (Ed.) *Characterization of macromolecular structure*, Publication 1573, National Academy of Sciences (U.S.A.), 1968, p. 261.
[7] H. Tompa. *Polymer Solutions*, Butterworths, London, 1956.
[8] P. J. Flory. *J. Chem. Phys.* **10**, 51 (1942); **12**, 425 (1944).
[9] P. J. Flory. *Principles of Polymer Chemistry*, Cornell University Press, 1953.
[10] M. L. Huggins. *Ann. N.Y. Acad. Sci.* **43**, 1 (1942).
[11] M. L. Huggins. *J. Am. Chem. Soc.* **64**, 1712 (1942).
[12] M. L. Huggins, *Physical Chemistry of High Polymers*, J. Wiley, New York, 1958.
[13] See A. J. Staverman. In S. Flügge (Ed.) *Encyclopedia of Physics*, Springer, Vol. XIII, 1962, p. 399.
[14] M. L. Huggins. *J. Am. Chem. Soc.* **86**, 3535 (1964).
[15] G. Delmas, D. Patterson and T. Somcynski. *J. Polymer Sci.* **57**, 59 (1962).
[16] D. Patterson *et al.*, *Polymer* **6**, 455 (1967); **8**, 503 (1967).
[17] R. Koningsveld, Ph.D. Thesis, Leyden University, 1967.
[18] R. Koningsveld and A. J. Staverman. *J. Polymer Sci.*, Part A2, **6**, 305, 325, 349, 367, 383 (1968).
[19] R. Koningsveld and A. J. Staverman. *Kolloid Z. & Z. Polymere* **218**, 114 (1967); **220**, 31 (1967).
[20] R. Koningsveld. *Adv. Colloid Interface Sci.* **2**, 151 (1968).
[21] G. Rehage and R. Koningsveld. *J. Polymer Sci.* Part B, **6**, 421 (1968).
[22] G. Rehage, H. J. Palmen, D. Möller and W. Wefers, IUPAC Symposium on Macromolecules, Toronto, September 1968.
[23] H. Tompa. *Trans. Farad. Soc.* **45**, 1142 (1949).
[24] L. H. Tung. *J. Polymer Sci.* **61**, 449 (1962).
[25] K. Šolc. *Coll. Czech. Chem. Comm.*, in press.
[26] H. Tompa. *Trans. Farad. Soc.* **46**, 970 (1950).
[27] K. Šolc, private communication.
[28] M. Gordon, H. A. G. Chermin and R. Koningsveld. *Macromolecules* **2**, 207 (1969)
[29] G. Rehage, D. Möller and O. Ernst. *Makromol. Chem.* **88**, 232 (1965).
[30] G. Rehage and D. Möller. *J. Polymer Sci., Part C*, **16**, 1787 (1967).
[31] R. Koningsveld. In D. McIntyre (Ed.) *Characterization of Macromolecular Structure*, N.A.S. Publication 1573, 1968, p. 172.
[32] M. Bohdanecky, IUPAC Symposium on Macromolecules, Tokyo, 1966.
[33] R. L. Scott. *Ind. Eng. Chem.* **45**, 2532 (1953).
[34] A. J. Staverman and J. Th. G. Overbeek. Discussion remark to ref. 3.
[35] M. Kubín. *Coll. Czech. Chem. Comm.* **32**, 1505 (1967).
[36] R. Koningsveld and A. J. Pennings. *Rec. Trav. Chim.* **83**, 552 (1964).
[37] A. J Pennings. *J. Polymer Sci., Part C*, **16**, 1799 (1967).
[38] A. J. Pennings and H. A. G. Chermin. Third Microsymposium, Prague, September 1968.
[39] A. Englert and H. Tompa. Third Microsymposium, Prague, September 1968.
[40] R. Koningsveld and K. Šolc. Third Microsymposium, Prague, September 1968.
[41] K. Šolc. Private communication.
[42] H. A. G. Chermin and R. Koningsveld, First Microsymposium, Prague, September 1967.
[43] Th. G. Scholte and R. Koningsveld. *Kolloid Z. & Z. Polymere* **218**, 58 (1967).
[44] G. Rehage and W. Wefers. *J. Polymer Sci., Part A2*, **6**, 1683 (1968).
[45] M. L. Huggins and H. Okamoto in ref. 5.
[46] D. McIntyre, A. M. Wims and J. H. O'Mara. *Polymer Preprints ACS*, **6**, 1037 (1965).